Metabolism of the tryptamine-derived new psychoactive substances 5-MeO-2-Me-DALT, 5-MeO-2-Me-ALCHT, and 5-MeO-2-Me-DIPT and their detectability in urine studied by GC-MS, LC-MSn, and LC-HR-MS/MS

Journal:	*Drug Testing and Analysis*
Manuscript ID	DTA-17-0077.R1
Wiley - Manuscript type:	Research Article
Date Submitted by the Author:	n/a
Complete List of Authors:	Caspar, Achim; Saarland University, Department of Experimental and Clinical Toxicology Gaab, Jonas; Saarland University, Department of Experimental and Clinical Toxicology Michely, Julian; Saarland University, Department of Experimental and Clinical Toxicology Brandt, Simon; School of Pharmacy & Biomolecular Sciences , Liverpool John Moores University Meyer, Markus; Universitat des Saarlandes, Exp. u. Clin. Toxicology Maurer, Hans; Saarland University, Department of Experimental and Clinical Toxicology
Keywords:	new psychoactive substances, tryptamines, metabolism, cytochrome-P450, LC-MSn, LC-HR-MS/MS
Abstract:	Many N,N-dialkylated tryptamines show psychoactive properties and were encountered as new psychoactive substances. The aims of the presented work were to study the phase I and II metabolism and the detectability in standard urine screening approaches (SUSA) of 5-methoxy-2-methyl-N,N-diallyltryptamine (5-MeO-2-Me-DALT), 5-methoxy-2-methyl-N-allyl-N-cyclohexyltryptamine (5-MeO-2-Me-ALCHT), and 5-methoxy-2-methyl-N,N-diisopropyltryptamine (5-MeO-2-Me-DIPT) using GC-MS, LC-MSn, and LC-HR-MS/MS. For metabolism studies, urine was collected over a 24-h period after administration of the compounds to male Wistar rats at 20 mg/kg body weight (BW). Phase I and II metabolites were identified after urine precipitation with acetonitrile by LC-HR-MS/MS. 5-MeO-2-Me-DALT (24 phase I and 12 phase II metabolites), 5-MeO-2-Me-ALCHT (24 phase I and 14 phase II metabolites), and 5-MeO-2-Me-DIPT (20 phase I and 11 phase II metabolites) were mainly metabolized by O-demethylation, hydroxylation, N-dealkylation, and combinations of them as well as by glucuronidation and sulfation of phase I metabolites. Incubations with mixtures of pooled human liver microsomes and cytosols (pHLM and pHLC) confirmed that the main metabolic reactions in humans and rats might be identical. Furthermore, initial CYP activity screenings revealed that CYP1A2, CYP2C19, CYP2D6, and CYP3A4 were involved in hydroxylation, CYP2C19

	and CYP2D6 in O-demethylation, and CYP2C19, CYP2D6, and CYP3A4 in N-dealkylation. For SUSAs, GC-MS, LC-MSn, and LC-HR-MS/MS were applied to rat urine samples after 1 or 0.1 mg/kg BW doses, respectively. In contrast to the GC-MS SUSA, both LC-MS SUSAs were able to detect an intake of 5-MeO-2-Me-ALCHT and 5-MeO-2-Me-DIPT via their metabolites following 1 mg/kg BW administrations and 5-MeO-2-Me-DALT following 0.1 mg/kg BW dosage.

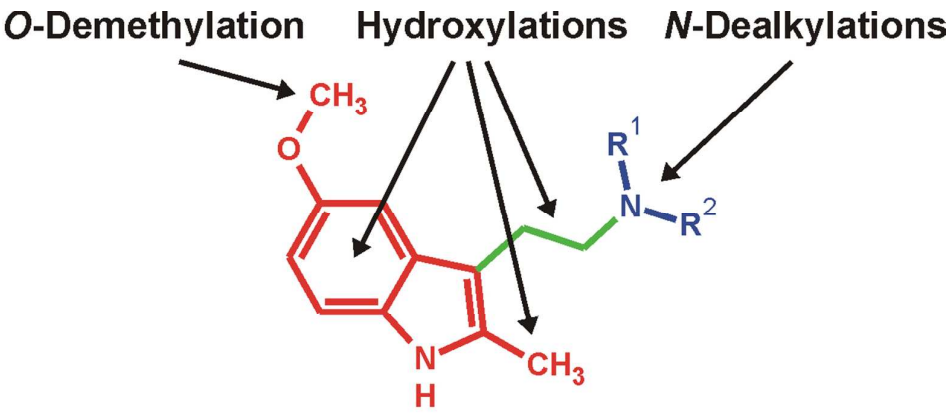

Graphical abstract

Metabolism of the tryptamine-derived new psychoactive substances 5-MeO-2-Me-DALT, 5-MeO-2-Me-ALCHT, and 5-MeO-2-Me-DIPT and their detectability in urine studied by GC-MS, LC-MS^n, and LC-HR-MS/MS

Achim T. Caspar,[a] Jonas B. Gaab,[a] Julian A. Michely,[a] Simon D. Brandt,[b,c] Markus R. Meyer,[a] Hans H. Maurer[a]*

Running Title: Metabolism of 5-MeO-2-Me-DALT, 5-MeO-2-Me-ALCHT, and 5-MeO-2-Me-DIPT

Number of text pages: 29

Number of figures: 4, 6 in supporting information

Number of tables: 7

---

[*]*Correspondence to: Hans H. Maurer, Department of Experimental and Clinical Toxicology, Saarland University, D-66421 Homburg (Saar), Germany,*

E-mail: hans.maurer@uks.eu, phone: +49-6841-16-26050, fax: +49-6841-16-26051.

[a] *Department of Experimental and Clinical Toxicology, Institute of Experimental and Clinical Pharmacology and Toxicology, Saarland University, D-66421 Homburg (Saar), Germany*

[b] *School of Pharmacy and Biomolecular Sciences, Liverpool John Moores University, James Parsons Building, Byrom Street, Liverpool L3 3AF, UK*

[c] *The Alexander Shulgin Research Institute, 1483 Shulgin Road, Lafayette, CA, 94549, USA*

Abstract

Many *N*,*N*-dialkylated tryptamines show psychoactive properties and were encountered as new psychoactive substances. The aims of the presented work were to study the phase I and II metabolism and the detectability in standard urine screening approaches (SUSA) of 5-methoxy-2-methyl-*N,N*-diallyltryptamine (5-MeO-2-Me-DALT), 5-methoxy-2-methyl-*N*-allyl-*N*-cyclohexyltryptamine (5-MeO-2-Me-ALCHT), and 5-methoxy-2-methyl-*N,N*-diisopropyltryptamine (5-MeO-2-Me-DIPT) using GC-MS, LC-MS^n, and LC-HR-MS/MS. For metabolism studies, urine was collected over a 24-h period after administration of the compounds to male Wistar rats at 20 mg/kg body weight (BW). Phase I and II metabolites were identified after urine precipitation with acetonitrile by LC-HR-MS/MS. 5-MeO-2-Me-DALT (24 phase I and 12 phase II metabolites), 5-MeO-2-Me-ALCHT (24 phase I and 14 phase II metabolites), and 5-MeO-2-Me-DIPT (20 phase I and 11 phase II metabolites) were mainly metabolized by *O*-demethylation, hydroxylation, *N*-dealkylation, and combinations of them as well as by glucuronidation and sulfation of phase I metabolites. Incubations with mixtures of pooled human liver microsomes and cytosols (pHLM and pHLC) confirmed that the main metabolic reactions in humans and rats might be identical. Furthermore, initial CYP activity screenings revealed that CYP1A2, CYP2C19, CYP2D6, and CYP3A4 were involved in hydroxylation, CYP2C19 and CYP2D6 in *O*-demethylation, and CYP2C19, CYP2D6, and CYP3A4 in *N*-dealkylation. For SUSAs, GC-MS, LC-MS^n, and LC-HR-MS/MS were applied to rat urine samples after 1 or 0.1 mg/kg BW doses, respectively. In contrast to the GC-MS SUSA, both LC-MS SUSAs were able to detect an intake of 5-MeO-2-Me-ALCHT and 5-MeO-2-Me-DIPT via their metabolites following 1 mg/kg BW administrations and 5-MeO-2-Me-DALT following 0.1 mg/kg BW dosage.

Keywords: new psychoactive substances; tryptamines; metabolism; cytochrome-P450; LC-MS^n; LC-HR-MS/MS

Introduction

New psychoactive substances (NPS) have become increasingly popular among drug users around the world.[1] As many of them are not regulated, these substances are marketed to avoid criminal prosecution for production, trading, drug possession, or consumption. NPS often mimic the effects of their traditional counterparts.[1] Several hundred substances are classified as NPS where research on the potential harm for consumers is limited. Synthetic cannabinoids, phenylethylamines, synthetic cathinones, and tryptamines were the most prevalent representatives of NPS during the last few years.[1] The biological effects associated with many psychoactive tryptamine derivatives are at least in part mediated by agonism at 5-HT_{1A} and 5-HT_{2A} receptors leading to hallucinogenic and stimulating effects.[2-7] The synthesis and mode of action for many synthetic tryptamines were described by Shulgin and Shulgin.[8] Examples of tryptamines described by them and subsequently appeared in case reports include 5-MeO-MIPT (5-methoxy-*N*-methyl-*N*-isopropyltryptamine)[9] and 5-MeO-DIPT (5-methoxy-*N*,*N*-diisopropyltryptamine).[10-14] Other tryptamines, such as 5-MeO-DALT (5-methoxy-*N*,*N*-diallyltryptamine),[15,16] originally not described by Shulgin and Shulgin in 1997,[8] have also appeared on the market and were linked to intoxication cases. Shulgin and Shulgin[8] have also described the effects of tryptamines substituted on the 2-position of the indole ring such as 5-MeO-TMT (5-methoxy-2,*N*,*N*-trimethyltryptamine). From this perspective, it seems conceivable that other 2-methylated tryptamines might also appear on the drug market. In cases of intoxication with such substances, it is necessary to provide analytical detection methods, such as standard urine screening approaches (SUSAs)[17] in order to facilitate adequate support of the therapeutic strategy used for clinical treatment. As shown by Michely *et al.*,[18] tryptamines were mainly excreted as metabolites thus the targets for urine screening have to be elucidated by metabolism studies to include those in SUSAs. This work here is focused on the metabolism and the detectability of the three NPS 5-methoxy-2-methyl-*N*,*N*-diallyltryptamine (5-MeO-2-Me-DALT), 5-methoxy-2-methyl-*N*-allyl-*N*-cyclohexyltryptamine (5-MeO-2-Me-ALCHT), and 5-methoxy-2-methyl-*N*,*N*-diisopropyltryptamine (5-MeO-2-Me-DIPT), respectively.

Experimental

Chemicals and reagents

5-MeO-2-Me-DALT, 5-MeO-2-Me-ALCHT, and 5-MeO-2-Me-DIPT were available from previous studies and synthesized by Brandt *et al.*[19-21] Isocitrate, isocitrate dehydrogenase, and 3'-phosphoadenosine-5'-phosphosulfate (PAPS) were received from Sigma-Aldrich (Taufkirchen, Germany), $NADP^+$ from Biomol (Hamburg, Germany), and methanol (LC-MS grade), ammonium formate (analytical grade), formic acid (LC-MS grade), and acetonitrile (LC-MS grade) and all other chemicals or reagents (analytical grade) from VWR (Darmstadt, Germany). The baculovirus-infected insect cell microsomes (supersomes) containing human cDNA-expressed cytochrome P450 (CYP) enzymes CYP1A2, CYP2A6, CYP2B6, CYP2C8, CYP2C9, CYP2C19, CYP2D6, CYP3A4 (1 nmol/mL, each), or CYP2E1, CYP3A5 (2 nmol/mL, each), pooled human liver microsomes (pHLM, 20 mg microsomal protein/mL, 330 pmol total CYP/mg protein), pooled human liver cytosols (pHLC, 20 mg cytosolic protein/mL), UDP-glucuronyltransferase (UGT) reaction mix solution A (25 mM UDP-glucuronic acid), and UGT reaction mix solution B (250 mM Tris-HCl, 40 mM $MgCl_2$, and 0.125 mg/mL alamethicin) were obtained from Corning (Amsterdam, The Netherlands). After delivery, the enzyme preparations were thawed at 37°C, aliquoted, snap-frozen in liquid nitrogen, and stored at -80°C until use.

Urine samples

The compounds were orally administered in an aqueous suspension by gastric intubation to male Wistar rats (Charles Rivers, Sulzfeld) for toxicological diagnostic reasons.[18] Doses were 20 mg/kg body weight (BW) for metabolism studies (identification of metabolites), 1 mg/kg BW for toxicological analyses, and 0.1 mg/kg BW for estimation of the detectability of very low dosed

applications, respectively. After administration, the rats were housed in metabolism cages for 24 h. Water was provided *ad libidum* and urine collected separately from feces. Before administration, blank urine samples were collected to evaluate the absence of interfering compounds. Urine samples were extracted, analyzed, and stored at -20°C immediately after collection.

Sample preparation for identification of phase I and II metabolites by LC-HR-MS/MS

As described elsewhere,[22] 100 µL urine were mixed with 500 µL acetonitrile, vortexed for 2 min and centrifuged for further 2 min at 10,000 *g*. Five hundred µL of the supernatant were transferred into a glass vial and evaporated at 70°C under a stream of nitrogen. The residue was dissolved in 50 µL of a mixture (1:1; *v*/*v*) of eluents A (2 mM aqueous ammonium formate plus 0.1% formic acid, pH 3) and B (2 mM aqueous ammonium formate with acetonitrile:methanol, 50:50, *v*/*v*; 1% water plus 0.1% formic acid) and a 1-µL aliquot was injected onto the LC-HR-MS/MS system.

Conditions for incubations for initial CYP activity screening studies

According to Richter *et al*.,[23] final concentrations of 25 µM substrate were used. The microsomal incubations were performed for 30 min at 37°C, each containing one of the following enzymes at 50 pmol/mL: CYP1A2, CYP2A6, CYP2B6, CYP2C8, CYP2C9, CYP2C19, CYP2D6, CYP2E1, CYP3A4, and CYP3A5. Further components in the final 50 µL incubation volume were phosphate buffer (90 mM, pH 7.4), 5 mM Mg^{2+}, 5 mM isocitrate, 1.2 mM $NADP^{+}$, 1.6 U/mL isocitrate dehydrogenase, and 200 U/mL superoxide dismutase. According to the Gentest manual, phosphate buffer was replaced with 45 and 90 mM Tris buffer for incubation of CYP2A6 and CYP2C19. Reactions were initiated by addition of the respective test substrate and stopped by addition of 50 µL ice-cold acetonitrile. The solution was then centrifuged for 5 min at 10,000 *g*, 70 µL of the supernatant were transferred to an autosampler vial, and 1 µL was injected onto the LC-HR-MS/MS

system. Blank and negative control samples were also prepared accordingly, whereby substrate or enzymes were replaced with buffer, respectively.

Conditions for incubations with pHLM + pHLC

As described by Richter *et al*.,[23] the *in vitro* drug metabolism studies using a mixture of pHLM and pHLC were done with final protein concentrations of 1 mg/mL each. After 10 min of preincubation at 37°C with 20 µL UGT reaction mix solution B, pHLM, pHLC, 90 mM phosphate buffer (pH 7.4), 2.5 mM Mg^{2+}, 2.5 mM isocitrate, 0.6 mM $NADP^{+}$, 0.8 U/mL isocitrate dehydrogenase, 100 U/mL superoxide dismutase, 10 µL UGT reaction mix A, and 40 µM aqueous PAPS were added. All given concentrations are final concentrations. The reaction was initiated by adding substrate at 25 µM (100 µL final volume) and stopped after 30 min incubation time with 50 µL ice-cold acetonitrile. The samples were centrifuged for 2 min at 10,000 *g*, 100 µL of the supernatant transferred into an autosampler vial, and 1 µL injected onto the LC-HR-MS/MS system. A blank and a negative control sample were also prepared, whereby substrate or enzyme was replaced with buffer, respectively.

LC-HR-MS/MS apparatus for identification of phase I and II metabolites in urine and incubations

The prepared samples were analyzed using a ThermoFisher Scientific (TF, Dreieich, Germany) Dionex UltiMate 3000 RS LC system, consisting of a degasser, a quaternary pump, and an UltiMate autosampler and coupled to a TF Q-Exactive Plus system equipped with heated electrospray ionization (HESI)-II source. The instrument was used in positive ionization mode. According to the manufacturer's manual, mass calibration was done before analysis using external mass calibration. LC and MS settings were according to published procedures.[23,24] The gradient elution was performed on a TF Accucore PhenylHexyl column (100 x 2.1 mm, 2.6 µm). Chromatographic

separation was performed at 40°C supplied by an analytical column heater (Dionex UltiMate 3000). The gradient was programmed as follows: 0-1 min 99% A, 1-10 min to 1% A, 10-11.5 min hold 1% A, and 11.5-13.5 min hold 99% A. The flow rate was set to 500 µL/min for 10 min and 800 µL/min from 10 to 13.5 min. The HESI-II source conditions were as follows: sheath gas, 60 arbitrary units (AU); auxiliary gas, 10 AU; spray voltage, 3.00 kV; heater temperature, 320°C; ion transfer capillary temperature, 320°C; and S-lens RF level, 60.0. Mass spectrometry analyses were performed using full-scan (FS) data and a subsequent data dependent acquisition (DDA) mode with an inclusion list of the *m/z* values of 5-MeO-2-Me-DALT, 5-MeO-2-Me-ALCHT, 5-MeO-2-Me-DIPT and their potential metabolites. Additional DDA without inclusion list was performed to detect unexpected metabolites. The settings for FS acquisition were as follows: resolution, 35,000; microscans, 1; automatic gain control (AGC) target, 1e6; maximum injection time (IT), 120 ms; and scan range, *m/z* 130-1000; loop count, 5; dynamic exclusion, 1 s. The settings for DDA mode were as follows: resolution, 17,500; microscans, 1; AGC target, 2e5; maximum IT, 250 ms; isolation window, 1.0 *m/z*, HCD with stepped normalized collision energy (NCE), 17.5, 35, and 52.5%; spectrum data type, profile; underfill ratio, 0.5% (corresponding to a signal with an abundance of 4e3); option exclude isotopes, enabled. Software for data evaluation was Thermo Fisher Xcalibur 2.2 SP1.48.

Standard urine screening approaches (SUSA)

The SUSAs were performed as described previously: GC-MS SUSA,[17,25] LC-MS^n SUSA,[26,27] and LC-HR-MS/MS SUSA.[26,28]

Results and discussion

Identification of phase I and II metabolites via LC-HR-MS/MS

Mass spectral interpretations were based on general fragmentation rules[29] and by comparison with the spectra of the parent compounds. All phase I and II metabolites tentatively identified based on their MS^2 spectra are depicted in Figures S1-S6 in Supporting Information (SI). Additionally, the spectra contain the supposed chemical structures, the accurate measured masses, the molecular formulae, and the corresponding mass error values in parts per million (ppm).

Proposed fragmentation patterns for identification of phase I metabolites via LC-HR-MS/MS

In general, all metabolites were identified based on their *m/z* values of the protonated molecule (PM), the calculated molecular formulae, and the fragmentation patterns compared to those of the parent compounds. They were sorted by PM and with abbreviations for the corresponding compound (5-MeO-2-Me-DALT, D; 5-MeO-2-Me-ALCHT, A; and 5-MeO-2-Me-DIPT, P). Due to the large number of metabolites detected in this study, only representative examples have been chosen to illustrate the fragmentation patterns. Following the suggestion described by Michely *et al*.,[18] the chemical structures were divided into three sections to allow a convenient description of fragmentation patterns and positions of metabolic reactions. Section 1 represents the aromatic ring system, section 2 the ethyl spacer, and section 3 the variable amine part of the molecule. As expected, the fragment ions formed by section 1 and 2 were the same for 5-MeO-2-Me-DALT, 5-MeO-2-Me-ALCHT, and 5-MeO-2-Me-DIPT. All masses in the following sections are the calculated (exact) masses.

5-MeO-2-Me-DALT

As shown in Figure S1 (see SI), 24 phase I metabolites of 5-MeO-2-Me-DALT could be identified. 5-MeO-2-Me-DALT (D1 in Figure S1; PM at *m/z* 285.1961, $C_{18}H_{25}ON_2^+$) showed a fragmentation comparable to DALT and 5-MeO-DALT[18] and for most of the detected metabolites. The fragment

ions of *m/z* 188.1070 ($C_{12}H_{14}ON^+$) and 110.0964 ($C_7H_{12}N^+$) represented typical α-cleavage of the tryptamine structure forming the characteristic fragment ions of sections 1 plus 2 (*m/z* 188.1070, $C_{12}H_{14}ON^+$) and section 3 (*m/z* 110.0964, $C_7H_{12}N^+$). The fragment ion of *m/z* 173.0835 ($C_{11}H_{11}ON^{\bullet+}$) resulted by a loss of a methyl radical of the methoxy group. For metabolite identification, the representative MS^2 fragment ions for section 3 were used in most cases. Unmodified section 3 led to a fragment ion of *m/z* 110.0964 ($C_7H_{12}N^+$), which suggested that the expected modification took place in sections 1 or 2. Modified section 3 led to fragment ions of *m/z* 70.0651 ($C_4H_8N^+$, *N*-deallylated) as shown e.g. in the MS^2 spectrum of *N*-deallyl-5-MeO-2-Me-DALT (D5, PM at *m/z* 245.1648, $C_{15}H_{21}ON_2^+$). As expected, the fragment ions of unchanged sections 1 and 2 (*m/z* 173.0835 and 188.1070) were also present. After *O*-demethylation, corresponding fragment ions of *m/z* 159.0679 ($C_{10}H_9ON^+$) and 174.0913 ($C_{11}H_{12}ON^+$), shown e.g. in the MS^2 spectrum of *O*-demethyl-5-MeO-2-Me-DALT (D11, PM at *m/z* 271.1805, $C_{17}H_{23}ON_2^+$), were detected, which was consistent with the detection of *m/z* 110.0964 ($C_7H_{12}N^+$). Furthermore, five isomers with the PM of *m/z* 301.1911, $C_{18}H_{25}O_2N_2^+$) could be observed and predicted to represent hydroxylated metabolites (D16-D20). Isomers 1-4 (D16-D19) showed fragment ions of *m/z* 110.0964 ($C_7H_{12}N^+$) indicating that the hydroxylation took place at sections 1 or 2. In the MS^2 spectrum of hydroxy-alkyl isomer 1 (D16), no specific shifts could be detected for the fragment ions (e.g. 188.1070 to 204.1019, +15.9949, +O) associated with sections 1 and 2 or any loss of water as in the MS^2 spectrum of hydroxy-alkyl isomer 2, which could indicate hydroxylation probably at the 2-methyl group of section 1. The fragment ions of *m/z* 176.0706 ($C_{10}H_{10}O_2N^+$) and 178.0863 ($C_{10}H_{12}O_2N^+$) represented a hydroxylated methyl group in section 1 with the positive charge at the carbon or at the nitrogen atom, respectively. In contrast, the MS^2 spectra of the hydroxy-aryl isomers 1 and 2 (D17 and D18) showed typical shifts of +15.9949 u (+O) of the fragment ions of sections 1 and 2, thus, resulting in the fragment ions of *m/z* 189.0784 ($C_{11}H_{11}O_2N^+$) and 204.1019 ($C_{12}H_{14}O_2N^+$). Furthermore, there were no fragment ions associated with a loss of water in these two spectra and thus the two isomers were predicted to be aryl hydroxylated metabolites (D17 and D18). In contrast, the MS^2 spectrum of hydroxy-alkyl isomer 2

(D19) showed such a loss of water (-18.0106 u, H_2O), typically observed with alkyl hydroxy groups, and therefore resulting in *m/z* 186.0913 ($C_{12}H_{12}ON^+$), which suggested that hydroxylation occurred in the ethylamine side chain in section 2. The MS^2 spectrum of isomer 5 (D20) showed neither presence of the fragment ion of unchanged section 3 (*m/z* 110.0964, ($C_7H_{12}N^+$), nor any typical shifts of this fragment ion. However, the fragment ions of unchanged sections 1 and 2 were detected and therefore the metabolite was inconsistent with a hydroxylated species. The presence of an *N*-oxide metabolite seemed likely as D20 had a longer retention time (5.0 min) than the parent compound (4.8 min) on the reversed phase column. This was observed for all *N*-oxides for which reference standards were available.[30]

5-MeO-2-Me-ALCHT and 5-MeO-2-Me-DIPT

According to Figures S3 and S5 (see SI), 24 phase I metabolites could be identified for 5-MeO-2-Me-ALCHT and 20 phase I metabolites for 5-MeO-2-Me-DIPT, respectively. As already mentioned above, the fragmentation patterns of the two parent compounds were comparable to those of 5-MeO-2-Me-DALT. The α-cleavages of 5-MeO-2-Me-ALCHT (A1 in Figure S3; PM at *m/z* 327.2431, $C_{21}H_{31}ON_2^+$) and 5-MeO-2-Me-DIPT (P1 in Figure S5; PM at *m/z* 289.2274, $C_{18}H_{29}ON_2^+$) formed the fragment ions of *m/z* 188.1070 ($C_{12}H_{14}ON^+$) representing sections 1 and 2 and *m/z* 152.1434 ($C_{10}H_{18}N^+$) and *m/z* 114.1277 ($C_7H_{16}N^+$), respectively, representing the iminium ion of section 3. In contrast to 5-MeO-2-Me-DALT, for both compounds a further breakdown of section 3 could be detected, forming the fragment ions of *m/z* 70.0651 ($C_4H_8N^+$) after loss of the cyclohexyl group and *m/z* 72.0807 ($C_4H_{10}N^+$) after loss of one isopropyl group. The metabolite formed after *N*,*N*-bis-dealkylation (*N*,*N*-bis-deallyl, D2; *N*-deallyl-*N*-decyclohexyl, A2; and *N*,*N*-bis-deisopropyl metabolite, P2) and the further deaminated and oxidized carboxy metabolite (D3, A3, and P3) were identical for all three compounds, representing the conserved 2-methyltryptamine structure. Furthermore, all metabolites formed after *N*-deallylation of 5-MeO-2-Me-DALT (D4-D10) and *N*-decyclohexylation of 5-MeO-2-Me-ALCHT (A4-A9) were identical for both

compounds, except for D7 which was only found after *N*-deallylation and oxidation of 5-MeO-2-Me-DALT.

Proposed fragmentation patterns for identification of phase II metabolites via LC-HR-MS/MS

5-MeO-2-Me-DALT

As shown in Figure S2 (see SI), all 12 identified phase II metabolites were conjugated at the indole part. The conjugates showed the same fragment ions as the underlying phase I metabolites after a characteristic elimination of glucuronic acid (-176.0321 u) of the glucuronides and of sulfuric acid (-79.9568 u) of the sulfates. The fragment ions of *m/z* 240.0325 ($C_{10}H_{10}O_4NS^+$), 254.0482 ($C_{11}H_{12}O_4NS^+$), and 284.0587 ($C_{12}H_{14}O_5NS^+$) formed after sulfation and the fragment ions of *m/z* 336.1078 ($C_{16}H_{18}O_7N^+$), 350.1234 ($C_{17}H_{20}O_7N^+$), 366.1183 ($C_{17}H_{20}O_8N^+$), and 380.1340 ($C_{18}H_{22}O_8N^+$) after glucuronidation at the ethylindole part (section 1 and 2) after *O*-demethylation or aryl-hydroxylation, respectively.

5-MeO-2-Me-ALCHT and 5-MeO-2-Me-DIPT

As shown in Figures S4 and S6 (see SI), 14 phase II metabolites of 5-MeO-2-Me-ALCHT and 11 of 5-MeO-2-Me-DIPT could be identified. As already described for 5-MeO-2-Me-DALT, all glucuronides and sulfates eliminated glucuronic acid (-176.0321 u) or sulfuric acid (-79.9568 u). In addition, conjugation always took place at the ethylindole part after *O*-demethylation or aryl-hydroxylation, forming the same fragment ions of the conjugated partial structure. As both compounds have some common phase I metabolites following *N*-dealkylation, the resulting phase II metabolites after further conjugation were consequently also identical (D6S, D8S, D4G, D6G, and $D8G_2$ for 5-MeO-2-Me-DALT; A6S, A9S, A4G, A6G, and A9G for 5-MeO-2-Me-ALCHT).

Proposed metabolic pathways

Based on the identified metabolites, the metabolic pathways for 5-MeO-2-Me-DALT, 5-MeO-2-Me-ALCHT, and 5-MeO-2-Me-DIPT were proposed and depicted in Figures 1-3. The numbering is given in Figures S1, S3, and S5 (see SI). As expected, the main metabolic reactions observed for all three test drugs were comparable.

5-MeO-2-Me-DALT

Four different hydroxy isomers could be detected. Two isomers of hydroxy-aryl (D17 and D18) were formed by hydroxylation at the indole part. Hydroxy-alkyl isomer 1 (D16) led to further oxidation and/or hydroxylation steps in section 1 (D15, D21, D22, and D23). Hydroxylation at section 2, forming hydroxy-alkyl isomer 2 (D19), was probably the preliminary step for the formation of two *N*-deallyl-oxo isomers 1 and 2 (D7 and D8). Moreover, *N*-oxidation (D20) alone and in combination with aryl hydroxylation (D24) was identified. The intermediate mono-hydroxy metabolite that led to the bis-hydroxylated product (both section 3; D25) was not detected. Initial *O*-demethylation (D11) and further oxidation led to *O*-demethyl-hydroxy-alkyl isomer 1 and 2 (D12 and D13) and *O*-demethyl-*N*-oxide (D14). Combination of *O*-demethylation and *N*-deallylation led to *O*-demethyl-*N*-deallyl metabolite (D4), following hydroxylation to *O*-demethyl-*N*-deallyl-hydroxy-alkyl (D6). After *N*-deallylation and further hydroxylation, two *N*-deallyl-hydroxy metabolites (D9, hydroxy-aryl and D10, hydroxy-alkyl) could be found. Finally, when D5 was further deallylated, a *N,N*-bis-deallyl metabolite (D2) was formed, that might have been deaminated and carboxylated to give *N,N*-bis-deallyl-deamino carboxylic acid (D3). Glucuronidation and sulfation could be observed for *O*-demethyl-*N*-deallyl (D4), *O*-demethyl-*N*-deallyl-hydroxy-alkyl (D6), *N*-deallyl-hydroxy-aryl (D9), *O*-demethyl (D11), and hydroxy-aryl isomer 2 (D18)

metabolites. For *O*-demethyl-hydroxy-alkyl isomer 2 (D13) and hydroxy-aryl isomer 1 (D17), only the glucuronidation species were detected.

5-MeO-2-Me-ALCHT

The metabolic pathways were similar to those observed for 5-MeO-2-Me-DALT including *N*-oxidation (A23), aliphatic (A20 and A21) and aromatic (A22) hydroxylation. However, aliphatic hydroxylations did not affect section 2 but the 2-methyl substituent in section 1 and the cyclohexyl ring in section 3 instead. Combination of both hydroxylation types (aromatic and aliphatic) showed the bis-hydroxy metabolite (A25). An intermediate biotransformation step (aliphatic hydroxylation at the 2-methyl substituent) was originally considered, but this could not be identified, possibly due to fast oxidation to the carboxylic acid (A24). In contrast to 5-MeO-2-Me-DALT and 5-MeO-2-Me-DIPT reflecting a symmetrical *N*,*N*-dialkylation pattern, 5-MeO-2-Me-ALCHT represents an asymmetrically substituted amine. In consequence, besides the comparable *O*-demethylation (A17) with further cyclohexyl hydroxylation (A18 and A19) and *N*-deallylation (A11), *N*-decyclohexylation (A5) was found to be an important metabolic step as well. *N*-decyclohexylation of 5-MeO-2-Me-ALCHT produced the same metabolite that resulted from *N*-deallylation of 5-MeO-2-Me-DALT. Similarly, additional transformations included hydroxylations (A8 and A9), oxidation to amide structure (A7), *O*-demethylation (A4), combinations of both (A6), and further *N*-deallylation (A2), followed by oxidation to the corresponding carboxylic acid (A3). Retention times and MS^2 spectra of these metabolites were the same for 5-MeO-2-Me-DALT and -ALCHT. However, the alpha-position in metabolites A7 and D8 is not the probable position due to fact that the intermediate should be an unstable hemiaminal. The *N*-deallylated metabolite (A11) could be further metabolized by hydroxylation (A15 and A16), oxidation to an aldehyde (D14), *O*-demethylation (A10), and combination of *O*-demethylation with hydroxylation (A12 and A13). Glucuronidation and sulfation were found for *O*-demethyl-*N*-decyclohexyl-hydroxy-alkyl (A6), *N*-decyclohexyl (A8), *O*-demethyl-*N*-deallyl (A10), *O*-demethyl-*N*-deallyl-hydroxy-cyclohexyl (A12),

O-demethyl (A17), and *O*-demethyl-hydroxy-cyclohexyl (A18) metabolites, whereas *O*-demethyl-*N*-decyclohexyl (A4) was only found as glucuronide. Two glucuronide isomers (A8G1 and A8G2) were detected for the *N*-decyclohexyl-hydroxy-aryl metabolite (A8).

5-MeO-2-Me-DIPT

As expected, most 5-MeO-2-Me-DIPT metabolites were found to be equivalent to those described above, such as aliphatic (P15 and P18) and aromatic (P16 and P17) hydroxylations, combination of aliphatic and aromatic hydroxylation (P21), oxidation to an aldehyde (P14), and the corresponding carboxylic acid (P19), *O*-demethylation (P11), and *N*-deisopropylation (P5). The aldehyde metabolite (P14) could be further oxidized forming hydroxy-alkyl-oxo metabolite (P20). Furthermore, *N,N*-bis-deisopropylation (P2) and deamination to the corresponding carboxylic acid (P3) leading to the same metabolites as already seen for the DALT (D2 and D3) and ALCHT (A2 and A3) analogue. Combinations of *N*-deisopropylation with hydroxylations (P9 and P10) and *O*-demethylation (P6) as well as combinations of *O*-demethylation with hydroxylations (P12 and P13), and *O*-demethylation with *N*-deisopropylation (P4) were discovered. *N*-Deisopropylation in combination with oxidation to two oxo isomers (P7 and P8) could also be found as for the DALT analogue (D7 and D8). Glucuronidation and sulfation could be observed for *O*-demethyl-*N*-deisopropyl (P4) and *O*-demethyl (P11) metabolites. For *O*-demethyl-*N*-deisopropyl-hydroxy-alkyl (P6), *N*-deisopropyl-hydroxy-aryl (P9), *O*-demethyl-hydroxy-alkyl isomer 2 (P13), hydroxy-aryl isomer 1 and 2 (P16 and P17), and aryl-alkyl-bis-hydroxy (P21) metabolites, only glucuronides were found. Two glucuronide isomers (P9G1 and P9G2) were detected for the *N*-deisopropyl-hydroxy-aryl metabolite (P9).

Comparison to published 5-MeO-DALT and 5-MeO-DIPT metabolism studies

5-MeO-2-Me-DALT

Michely *et al.*,[18] described the metabolism of 5-MeO-DALT in rats. The main metabolic reactions (*O*-demethylation, hydroxylations, and *N*-deallylation) were similar for both compounds. However, some metabolites, especially those modified at the 2-methyl group could only be found for 5-MeO-2-Me-DALT. Compared to 5-MeO-DALT, no bis- or tris-hydroxylations and no ring-rearranged metabolite could be found for the 2-methyl derivative probably due to the substitution of the 2 position of the indole ring which could lead to a steric hindrance for the rearrangement. In addition, *N,N*-bis-deallylation followed by oxidative deamination and *N*-oxidation could only be detected for 5-MeO-2-Me-DALT.

5-MeO-2-Me-DIPT

Narimatsu *et al.*,[31-33] described, besides CYP kinetic studies, only the presence of a *O*-demethylated, a *N*-deisopropylated, and a mono-hydroxylated metabolite in rat and human liver microsomes, which all were also found in our study for 5-MeO-2-Me-DIPT.

Initial CYP activity screening studies

The ten most abundant human hepatic CYPs were incubated as described above to provide a qualitative description of metabolizing isoenzymes. As shown in Table 1, the involved isoenzymes were the same for the three NPS. *O*-Demethylation was catalyzed by CYP2C19 and CYP2D6, *N*-deallylation, or *N*-deisopropylation by CYP2C19, CYP2D6, and CYP3A4, and hydroxylations by CYP1A2, CYP2C19, CYP2D6, and CYP3A4. Additionally, the *N*-decyclohexylation of 5-MeO-2-Me-ALCHT was catalyzed by CYP2C9, CYP2C19, and CYP3A4.

Incubations with pHLM and pHLC

Due to the lack of authentic human urine samples, *in vitro* testing was performed to evaluate the transferability of rat metabolism results to humans. The combination of rat urine studies and the incubation of pHLM and/or pHLC with the corresponding cofactors is a common technique that produced reliable results and data for detection methods in human urine as shown in previous studies.[23,34-37] However, it should be kept in mind, that the comparison of *in vitro* and *in vivo* models could be challenging due to sampling time of urine (24 h), time, amount, and route of application, the used incubation conditions, and/or genetic variations.

5-MeO-2-Me-DALT

As summarized in Table 2, 22 out of 24 identified phase I metabolites of 5-MeO-2-Me-DALT were detected in rat urine, 14 could be confirmed in the *in vitro* approach. In addition, two hydroxy-alkyl metabolites (D16 and D19) were only detected in the *in vitro* model. This was probably based on the 24 hours urine collection period and consequently further metabolism steps to the corresponding oxo or carboxy metabolites occurred in rat. D4, D6, D9, D11, D13, D17, and D18 were found as glucuronides, and D4, D6, D9, D11, and D18 as sulfates *in vivo*. D11, D17, and D18 were found as glucuronides and D18 as sulfate *in vitro*. These differences could have been based on the incubation time and lower formation of the corresponding phase I metabolites, especially in cases where multiple metabolic reaction steps were needed.

5-MeO-2-Me-ALCHT

As shown in Table 3, 17 out of 24 identified *in vivo* phase I metabolites of 5-MeO-2-Me-ALCHT could be recovered from the *in vitro* model. Eight glucuronides and six sulfates were detected in rat urine and one glucuronide under *in vitro* conditions. The reasons for these differences were considered comparable to those mentioned above. In comparison to 5-MeO-2-Me-DALT, no additional metabolites could be found in the *in vitro* model when compared to the *in vivo* approach.

5-MeO-2-Me-DIPT

According to Table 4, 15 out of 20 phase I metabolites identified *in vivo* could also be found in the *in vitro* model. Nine glucuronides and two sulfates were identified *in vivo*, whereas two glucuronides were detected *in vitro*.

Toxicological detection by standard urine screening approaches (SUSAs)

So far, no data about dosages or potency of the compounds are available. Therefore, the tested dosages for 5-MeO-2-Me-DALT, 5-MeO-2-Me-ALCHT, and 5-MeO-2-Me-DIPT were estimated based on those described for other tryptamine-derived NPS and were set to 1 mg/kg BW and 0.1 mg/kg BW. Michely *et al.*[18] showed that such dosages were at or below common users doses of DALT and 5-MeO-DALT. The fact that the 0.1 mg/kg BW dosage was not detectable (except of 5-MeO-2-Me-DALT) could lead to a false negative result e.g. in context of forensic issues.

GC-MS SUSA

Unfortunately, the three compounds and/or their metabolites could not be detected in rat urine after low dosages probably due to low concentration or instabilities caused by the sample preparation. However, after high dose administration, some metabolites were detected, indicating that the compounds might be detectable in a case of acute overdose.

LC-MS^n SUSA

A list of all detected metabolites is given in Tables 5 and 6. 5-MeO-2-Me-DALT was detectable *via* its metabolites after both low dose administrations. For 5-MeO-2-Me-ALCHT as well as 5-MeO-2-Me-DIPT, only metabolites were detectable after 1 mg/kg BW dosages, but not after the lower 0.1 mg/kg BW dosages.

LC-HR-MS/MS SUSA

As summarized in Table 7, metabolites of 5-MeO-2-Me-DALT and 5-MeO-2-Me-DIPT could be identified with the accurate PM and a HR-MS/MS spectrum (identification, I) after 1 mg/kg BW dose administrations. In addition, metabolites could be identified after the lower 0.1 mg/kg BW dosage for 5-MeO-2-Me-DALT. For 5-MeO-2-Me-ALCHT, only detection (D) of the accurate PM without the corresponding HR-MS/MS spectrum was possible. A second run with an inclusion list on the masses of described metabolites would be necessary to confirm an intake of 5-MeO-2-Me-ALCHT. The parent compounds were not identified, nor have they been detected in any of the urine samples. Exemplified for 5-MeO-2-Me-DALT, Figure 4 shows a reconstituted ion chromatogram of the 1 mg/kg BW dosage rat urine sample with various detected metabolites.

Conclusions

5-MeO-2-Me-DALT, 5-MeO-2-Me-ALCHT, and 5-MeO-2-Me-DIPT were extensively metabolized in rats. *In vitro* metabolism studies with pHLM plus pHLC showed similar results, which indicated that the described metabolites should also be detectable in human urine samples. CYP1A2, CYP2C9, CYP2C19, CYP2D6, and CYP3A4 were identified to be involved in the biotransformation described in this study. An intake of an estimated users' dose of 1 mg/kg BW was detectable *via* the metabolites by both LC-MS SUSAs for 5-MeO-2-Me-DALT and 5-MeO-2-Me-DIPT. For 5-MeO-2-Me-ALCHT, a separate run using an inclusion list on the targets of interest

would be necessary for detection. In addition, 5-MeO-2-Me-DALT metabolites were also detectable after the lower 0.1 mg/kg BW dosage by both LC-MS SUSAs.

Acknowledgements

The authors would like to thank Sascha K. Manier, Lilian H. J. Richter, Lea Wagmann, Carsten Schröder, Gabriele Ulrich, and Armin A. Weber for support and/or helpful discussion.

References

[1] United Nations Office on Drugs and Crime (UNODC), *World Drug Report 2016*, https://www.unodc.org/doc/wdr2016/WORLD_DRUG_REPORT_2016_web.pdf, **2016.**

[2] N.V. Cozzi, P.F. Daley. Receptor binding profiles and quantitative structure-affinity relationships of some 5-substituted-N,N-diallyltryptamines. *Bioorg. Med. Chem. Lett.* **2016,** *26*, 959.

[3] A.L. Halberstadt, M.A. Geyer. Multiple receptors contribute to the behavioral effects of indoleamine hallucinogens. *Neuropharmacology* **2011,** *61*, 364.

[4] A. Rickli, O.D. Moning, M.C. Hoener, M.E. Liechti. Receptor interaction profiles of novel psychoactive tryptamines compared with classic hallucinogens. *Eur. Neuropsychopharmacol.* **2016,** *26*, 1327.

[5] T.S. Ray. Psychedelics and the human receptorome. *PLoS. One.* **2010,** *5*, e9019

[6] D.E. Nichols. Structure-activity relationships of serotonin 5-HT_{2A} agonists. *WIREs Membr. Transp. Signal* **2012,** *1*, 559.

[7] D.E. Nichols. Hallucinogens. *Pharmacol. Ther.* **2004,** *101*, 131.

[8] A. Shulgin, A. Shulgin, *Tihkal, The Continuation*, Transform Press, Berkley (CA), **1997.**

[9] E. Shimizu, H. Watanabe, T. Kojima, H. Hagiwara, M. Fujisaki, R. Miyatake, K. Hashimoto, M. Iyo. Combined intoxication with methylone and 5-MeO-MIPT. *Prog. Neuropsychopharmacol. Biol Psychiatry* **2007,** *31*, 288.

[10] R. Meatherall, P. Sharma. Foxy, a designer tryptamine hallucinogen. *J. Anal. Toxicol.* **2003,** *27*, 313.

[11] Y. Fuse-Nagase, T. Nishikawa. Prolonged delusional state triggered by repeated ingestion of aromatic liquid in a past 5-methoxy-N, N-diisopropyltryptamine abuser. *Addict. Sci. Clin. Pract.* **2013,** *8*, 9

[12] S.C. Smolinske, R. Rastogi, S. Schenkel. Foxy methoxy: a new drug of abuse. *J Med. Toxicol.* **2005,** *1*, 22.

[13] E. Tanaka, T. Kamata, M. Katagi, H. Tsuchihashi, K. Honda. A fatal poisoning with 5-methoxy-N,N-diisopropyltryptamine, Foxy. *Forensic Sci Int* **2006,** *163*, 152.

[14] J.M. Wilson, F. McGeorge, S. Smolinske, R. Meatherall. A foxy intoxication. *Forensic Sci Int* **2005,** *148*, 31.

[15] J.M. Corkery, E. Durkin, S. Elliott, F. Schifano, A.H. Ghodse. The recreational tryptamine 5-MeO-DALT (N,N-diallyl-5-methoxytryptamine): a brief review. *Prog. Neuropsychopharmacol. Biol. Psychiatry* **2012,** *39*, 259.

[16] A. Jovel, A. Felthous, A. Bhattacharyya. Delirium due to intoxication from the novel synthetic tryptamine 5-MeO-DALT. *J. Forensic Sci.* **2014,** *59*, 844.

[17] H.H. Maurer, K. Pfleger, A.A. Weber, *Mass spectral data of drugs, poisons, pesticides, pollutants and their metabolites*, Wiley-VCH, Weinheim (Germany), **2016.**

[18] J.A. Michely, A.G. Helfer, S.D. Brandt, M.R. Meyer, H.H. Maurer. Metabolism of the new psychoactive substances N,N-diallyltryptamine (DALT) and 5-methoxy-DALT and their detectability in urine by GC-MS, LC-MSn, and LC-HR-MS/MS. *Anal Bioanal. Chem.* **2015,** *407*, 7831.

[19] S.D. Brandt, R. Tearavarich, N. Dempster, N.V. Cozzi, P.F. Daley. Synthesis and characterization of 5-methoxy-2-methyl-N,N-dialkylated tryptamines. *Drug Test. Anal.* **2012,** *4*, 24.

[20] R. Tearavarich, V. Hahnvajanawong, N. Dempster, P.F. Daley, N.V. Cozzi, S.D. Brandt. Microwave-accelerated preparation and analytical characterization of 5-ethoxy-N,N-dialkyl-[alpha,alpha,beta,beta-H(4)]- and [alpha,alpha,beta,beta-D(4)]-tryptamines. *Drug Test. Anal.* **2011,** *3*, 597.

[21] S.D. Brandt, P.V. Kavanagh, G. Dowling, B. Talbot, F. Westphal, M.R. Meyer, H.H. Maurer, A.L. Halberstadt. Analytical characterization of N,N-diallyltryptamine (DALT) and 16 ring-substituted derivatives. *Drug Test. Anal.* **2017,** *9*, 115.

[22] D.K. Wissenbach, M.R. Meyer, D. Remane, A.A. Weber, H.H. Maurer. Development of the first metabolite-based LC-MSn urine drug screening procedure - exemplified for antidepressants. *Anal. Bioanal. Chem.* **2011,** *400*, 79.

[23] L.H.R. Richter, Y.R. Kaminski, F. Noor, M.R. Meyer, H.H. Maurer. Metabolic fate of desomorphine elucidated using rat urine, pooled human liver preparations, and human hepatocyte cultures as well as its detectability using standard urine screening approaches. *Anal. Bioanal. Chem.* **2016,** *408*, 6283.

[24] A.G. Helfer, A. Turcant, D. Boels, S. Ferec, B. Lelievre, J. Welter, M.R. Meyer, H.H. Maurer. Elucidation of the metabolites of the novel psychoactive substance 4-methyl-*N*-ethyl-cathinone (4-MEC) in human urine and pooled liver microsomes by GC-MS and LC-HR-MS/MS techniques and of its detectability by GC-MS or LC-MS^n standard screening approaches. *Drug Test. Anal.* **2015,** *7*, 368.

[25] M.R. Meyer, C. Lindauer, J. Welter, H.H. Maurer. Dimethocaine, a synthetic cocaine derivative: Studies on its in vivo metabolism and its detectability in urine by LC-HR-MS^n and GC-MS using a rat model. *Anal. Bioanal. Chem.* **2014,** *406*, 1845.

[26] A.T. Caspar, A.G. Helfer, J.A. Michely, V. Auwaerter, S.D. Brandt, M.R. Meyer, H.H. Maurer. Studies on the metabolism and toxicological detection of the new psychoactive

designer drug 2-(4-iodo-2,5-dimethoxyphenyl)-N-[(2-methoxyphenyl)methyl]ethanamine (25I-NBOMe) in human and rat urine using GC-MS, LC-MSn, and LC-HR-MS/MS. *Anal. Bioanal. Chem.* **2015,** *407*, 6697.

[27] D.K. Wissenbach, M.R. Meyer, D. Remane, A.A. Philipp, A.A. Weber, H.H. Maurer. Drugs of abuse screening in urine as part of a metabolite-based LC-MS(n) screening concept. *Anal. Bioanal. Chem.* **2011,** *400*, 3481.

[28] A.G. Helfer, J.A. Michely, A.A. Weber, M.R. Meyer, H.H. Maurer. Orbitrap technology for comprehensive metabolite-based liquid chromatographic-high resolution-tandem mass spectrometric urine drug screening - exemplified for cardiovascular drugs. *Anal. Chim. Acta* **2015,** *891*, 221.

[29] W.M.A. Niessen. Fragmentation of Toxicologically Relevant Drugs in Positive-Ion Liquid Chromatography-Tandem Mass Spectrometry. *Mass Spectrometry Reviews* **2011,** *30*, 626.

[30] H.H. Maurer, M.R. Meyer, A.G. Helfer, A.A. Weber, *Maurer/Meyer/Helfer/Weber MMHW LC-HR-MS/MS library of drugs, poisons, and their metabolites*, Wiley-VCH, Weinheim (Germany), **2017.**

[31] M.J. Jin, C. Jin, J.Y. Kim, M.K. In, O.S. Kwon, H.H. Yoo. A quantitative method for simultaneous determination of 5-methoxy-N,N-diisopropyltryptamine and its metabolites in urine using liquid chromatography-electrospray ionization-tandem mass spectrometry. *J. Forensic Sci.* **2011,** *56*, 1044.

[32] S. Narimatsu, R. Yonemoto, K. Saito, K. Takaya, T. Kumamoto, T. Ishikawa, M. Asanuma, M. Funada, K. Kiryu, S. Naito, Y. Yoshida, S. Yamamoto, N. Hanioka. Oxidative metabolism of 5-methoxy-N,N-diisopropyltryptamine (Foxy) by human liver microsomes and recombinant cytochrome P450 enzymes. *Biochem. Pharmacol.* **2006,** *71*, 1377.

[33] S. Narimatsu, R. Yonemoto, K. Masuda, T. Katsu, M. Asanuma, T. Kamata, M. Katagi, H. Tsuchihashi, T. Kumamoto, T. Ishikawa, S. Naito, S. Yamano, N. Hanioka. Oxidation of 5-methoxy-N,N-diisopropyltryptamine in rat liver microsomes and recombinant cytochrome P450 enzymes. *Biochem. Pharmacol.* **2008,** *75*, 752.

[34] M.R. Meyer, S. Mauer, G.M.J. Meyer, J. Dinger, B. Klein, F. Westphal, H.H. Maurer. The in vivo and in vitro metabolism and the detectability in urine of 3',4'-methylenedioxy-alpha-pyrrolidinobutyrophenone (MDPBP), a new pyrrolidinophenone-type designer drug, studied by GC-MS and LC-MSn. *Drug Test. Anal.* **2014,** *6*, 746.

[35] J. Welter, P. Kavanagh, M.R. Meyer, H.H. Maurer. Benzofuran analogues of amphetamine and methamphetamine: studies on the metabolism and toxicological analysis of 5-APB and 5-MAPB in urine and plasma using GC-MS and LC-(HR)-MS^n techniques. *Anal. Bioanal. Chem.* **2015,** *407*, 1371.

[36] A.T. Caspar, S.D. Brandt, A.E. Stoever, M.R. Meyer, H.H. Maurer. Metabolic fate and detectability of the new psychoactive substances 2-(4-bromo-2,5-dimethoxyphenyl)-N-[(2-methoxyphenyl)methyl]ethanamine (25B-NBOMe) and 2-(4-chloro-2,5-dimethoxyphenyl)-N-[(2-methoxyphenyl)methyl]ethanamine (25C-NBOMe) in human and rat urine by GC-MS, LC-MS^n, and LC-HR-MS/MS approaches. *J. Pharm. Biomed. Anal.* **2017,** *134*, 158.

[37] M. Katagi, T. Kamata, K. Zaitsu, N. Shima, H. Kamata, K. Nakanishi, H. Nishioka, A. Miki, H. Tsuchihashi. Metabolism and toxicologic analysis of tryptamine-derived drugs of abuse. *Ther. Drug Monit.* **2010,** *32*, 328.

Table 1 CYP isoenzymes involved in metabolic pathways of 5-MeO-2-Me-DALT, 5-MeO-2-Me-ALCHT, and 5-MeO-2-Me-DIPT

Pathway	CYP 1A2	CYP 2A6	CYP 2B6	CYP 2C8	CYP 2C9	CYP 2C19	CYP 2D6	CYP 2E1	CYP 3A4	CYP 3A5
5-MeO-2-Me-DALT										
O-Demethylation						+	+			
N-Deallylation						+	+		+	
Hydroxylations	+					+	+		+	
5-MeO-2-Me-ALCHT										
O-Demethylation						+	+			
N-Deallylation						+	+		+	
N-Decyclohexylation					+	+			+	
Hydroxylations	+					+	+		+	
5-MeO-2-Me-DIPT										
O-Demethylation						+	+			
N-Deisopropylation	+					+	+		+	
Hydroxylations	+					+	+		+	

Table 2 Appearance of 5-MeO-2-Me-DALT phase I and II metabolites in rat urine and in pHLM/HLC mix; G = glucuronide, S = sulfate; numbering according to Figure S1 (see SI).

Metabolite	Rat urine		pHLM/HLC	
	Phase I	Phase II	Phase I	Phase II
D2	+			
D3	+			
D4	+	+ G/S	+	
D5	+		+	
D6	+	+ G/S	+	
D7	+			
D8	+			
D9	+	+ G/S	+	
D10	+		+	
D11	+	+ G/S	+	+ G
D12	+		+	
D13	+	+ G	+	
D14	+			
D15	+		+	
D16			+	
D17	+	+ G		+ G
D18	+	+ G/S	+	+ G/S
D19			+	
D20	+		+	
D21	+		+	
D22	+		+	
D23	+			
D24	+			
D25	+		+	

Table 3 Appearance of 5-MeO-2-Me-ALCHT phase I and II metabolites in rat urine and in pHLM/HLC mix; G = glucuronide, G_1/G_2 = glucuronide isomer 1 and 2, S = sulfate; numbering according to Figure S3 (see SI).

Metabolite	Rat urine		pHLM/HLC	
	Phase I	Phase II	Phase I	Phase II
A2	+			
A3	+			
A4	+	+ G	+	
A5	+		+	
A6	+	+ G/S	+	
A7	+			
A8	+	+ G_1/G_2/S	+	
A9	+		+	
A10	+	+ G/S	+	
A11	+		+	
A12	+	+ G/S		
A13	+		+	
A14	+			
A15	+			
A16	+		+	
A17	+	+ G/S	+	+ G
A18	+	+ G/S	+	
A19	+		+	
A20	+		+	
A21	+		+	
A22	+		+	
A23	+		+	
A24	+			
A25	+		+	

Table 4 Appearance of 5-MeO-2-Me-DIPT phase I and II metabolites in rat urine and in pHLM/HLC mix; G = glucuronide, G_1/G_2 = glucuronide isomer 1 and 2, S = sulfate; numbering according to Figure S5 (see SI).

Metabolite	Rat urine		pHLM/HLC	
	Phase I	Phase II	Phase I	Phase II
P2	+			
P3	+			
P4	+	+ G/S	+	
P5	+		+	
P6	+	+ G		
P7	+			
P8	+			
P9	+	+ G_1/G_2	+	
P10	+		+	
P11	+	+ G/S	+	+ G
P12	+		+	
P13	+	+ G	+	
P14	+		+	
P15	+		+	
P16	+	+ G	+	+ G
P17	+	+ G	+	
P18	+		+	
P19	+		+	
P20	+		+	
P21	+	+ G	+	

Table 5 Metabolites of 5-MeO-2-Me-DALT, *m/z* values of protonated molecule, characteristic MS^2 and MS^3 fragment ions, and retention time (RT) detected by LC-MS^n SUSA in both low dose urines (1 mg/kg BW and 0.1 mg/kg BW). The numbers correspond to those shown in Figures S1 and S2 (see SI).

No.	Target for SUSA	Protonated molecule, *m/z*	MS^2 fragment ions, *m/z*, and relative intensity, %	MS^3 fragment ions, *m/z*, and relative intensity, %, on the ion given in bold	RT, min
D4	5-MeO-2-Me-DALT-M (*O*-demethyl-*N*-deallyl-)	231	174 (100)	**174:** 146 (100), 133 (23), 131 (8)	4.3
D11	5-MeO-2-Me-DALT-M (*O*-demethyl-)	271	174 (100), 110 (4)	**174:** 146 (100), 133 (10), 131 (10)	6.2
D11 G	5-MeO-2-Me-DALT-M (*O*-demethyl-) glucuronide	447	350 (100), 271 (74), 174 (79)	**350:** 174 (100), 253 (26), 146 (2)	4.5
D13 G	5-MeO-2-Me-DALT-M (*O*-demethyl-HO-allyl-aryl-) glucuronide	463	366 (100), 190 (6)	**366:** 190 (100), 172 (4)	4.6
D17 G	5-MeO-2-Me-DALT-M (*O*-demethyl-HO-allyl-aryl-) glucuronide	477	380 (100), 204 (18), 301 (7)	**380:** 204 (100), 172 (7)	5.0

Table 6 Metabolites of 5-MeO-2-Me-ALCHT and 5-MeO-2-Me-DIPT, *m/z* values of protonated molecule, characteristic MS^2 and MS^3 fragment ions, and retention time (RT) detected by LC-MS^n SUSA in low dose urine (1 mg/kg BW). The numbers correspond to those shown in Figures S3-S6 (see SI).

No.	Target for SUSA	Protonated molecule, *m/z*	MS^2 fragment ions, *m/z*, and relative intensity, %	MS^3 fragment ions, *m/z*, and relative intensity, %, on the ion given in bold	RT, min
A10 G	5-MeO-2-Me-ALCHT-M (*O*-demethyl-*N*-deallyl-) glucuronide	449	174 (100), 273 (99),350 (20), 159 (13)	**174:** 146 (100) **273:** 174 (100)	6.1
A17 G	5-MeO-2-Me-ALCHT-M (*O*-demethyl-) glucuronide	489	350 (100), 313 (85), 174 (84), 152 (3)	**350:** 174 (100)	7.6
P11	5-MeO-2-Me-DIPT-M (*O*-demethyl-)	275	174 (100), 114 (4)	**114:** 72 (100) **174:** 146 (100), 131 (13) 133 (9)	6.0
P20	5-MeO-2-Me-DIPT-M (HO-alkyl-oxo-)	319	218 (100), 114 (6)	**218:** 190 (100), 186 (98),172 (75),158 (55)	6.6
P21	5-MeO-2-Me-DIPT-M (HO-alkyl-HO-aryl-)	321	220 (100), 205 (3), 114 (1)	**220:** 172 (100), 186 (98),190 (85), 160 (68),174 (27)	9.2
P11 G	5-MeO-2-Me-DIPT-M (*O*-demethyl-) glucuronide	451	350 (100), 174 (68), 275 (38)	**174:** 146 (100), 131 (11),133 (5)	4.3
P13 G	5-MeO-2-Me-DIPT-M (*O*-demethyl-HO-alkyl-) glucuronide	467	366 (100), 190 (76)	**190:** 134 (100) **366:** 190 (100), 172 (4)	4.2
P16 G	5-MeO-2-Me-DIPT-M (HO-aryl-) glucuronide isomer 1	481	380 (100), 204 (11)	**204:** 172 (100), 204 (5)	4.6
P17 G	5-MeO-2-Me-DIPT-M (HO-aryl-) glucuronide isomer 2	481	380 (100), 204 (30)	**204:** 173 (100), 172 (82), 163 (54), 204 (16)	5.4

Table 7 Metabolites of 5-MeO-2-Me-DALT, 5-MeO-2-Me-ALCHT, and 5-MeO-2-Me-DIPT, calculated exact mass of the protonated molecule, and retention time (RT) detected by LC-HR-MS/MS SUSA in rat urine (1 mg/kg body weight (BW) or 0.1 mg/kg BW). D = detection of protonated molecule in MS^1, I = identification via MS^1 and MS^2; the numbers correspond to those shown in Figures S1-S6 (see SI).

No.	Target for SUSA	Calculated exact masses of protonated molecule, *m/z*	1 mg/kg BW dose	0.1 mg/kg BW dose	RT, min
D4	5-MeO-2-Me-DALT-M (*O*-demethyl-*N*-deallyl-)	231.1492	I	I	3.0
D6	5-MeO-2-Me-DALT-M (*O*-demethyl-*N*-deallyl-HO-alkyl-)	247.1441	D	D	2.6
D11	5-MeO-2-Me-DALT-M (*O*-demethyl-)	271.1805	I	I	3.6
D13	5-MeO-2-Me-DALT-M (*O*-demethyl-HO-alkyl-) isomer 2	287.1754	I		3.3
D17	5-MeO-2-Me-DALT-M (HO-aryl-) isomer 1	301.1911	D	D	3.8
D18	5-MeO-2-Me-DALT-M (HO-aryl-) isomer 2	301.1911	I		4.0
D21	5-MeO-2-Me-DALT-M (HOOC-)	315.1703	D		3.7
D11 S	5-MeO-2-Me-DALT-M (*O*-demethyl-) sulfate	351.1373	D		3.8
D4 G	5-MeO-2-Me-DALT-M (*O*-demethyl-*N*-deallyl-) glucuronide	407.1813	D	D	2.7
D11 G	5-MeO-2-Me-DALT-M (*O*-demethyl-) glucuronide	447.2123	I	I	3.3
D17 G	5-MeO-2-Me-DALT-M (HO-aryl-) glucuronide	477.2231	D	D	3.4
A17	5-MeO-2-Me-ALCHT-M (*O*-demethyl-)	313.2274	D		4.9
A8 G_1	5-MeO-2-Me-ALCHT-M (*N*-decyclohexyl-HO-aryl-) glucuronide isomer 1	437.2282	D		3.1
A10 G	5-MeO-2-Me-ALCHT-M (*O*-demethyl-*N*-deallyl-) glucuronide	449.2282	D		3.8
A17 G	5-MeO-2-Me-ALCHT-M (*O*-demethyl-) glucuronide	489.2595	D		4.3
P4	5-MeO-2-Me-DIPT-M (*O*-demethyl-*N*-deisopropyl-)	233.1648	I		3.1
P11	5-MeO-2-Me-DIPT-M (*O*-demethyl-)	275.2118	I		3.7
P12	5-MeO-2-Me-DIPT-M (*O*-demethyl-HO-alkyl-) isomer 1	291.2067	I		2.8
P20	5-MeO-2-Me-DIPT-M (HOOC-)	319.2016	D		3.9
P4	5-MeO-2-Me-DIPT-M	409.1969	D		2.8

G	(*O*-demethyl-*N*-deisopropyl-) glucuronide				
P11 G	5-MeO-2-Me-DIPT-M (*O*-demethyl-) glucuronide	451.2439	D		3.2
P13 G	5-MeO-2-Me-DIPT-M (*O*-demethyl-HO-alkyl-) glucuronide	467.2389	D		3.2

Legends to Figures

Figure 1 Proposed metabolic pathways of 5-MeO-2-Me-DALT. Phase II metabolites: glucuronides (G), and sulfates (S). Structures in brackets represent proposed (but not detected) intermediates; numbering according to Figure S1 (see SI).

Figure 2 Proposed metabolic pathways of 5-MeO-2-Me-ALCHT. Phase II metabolites: glucuronides (G), and sulfates (S). Structures in brackets represent proposed (but not detected) intermediates; numbering according to Figure S3 (see SI).

Figure 3 Proposed metabolic pathways of 5-MeO-2-Me-DIPT. Phase II metabolites: glucuronides (G), and sulfates (S). Structures in brackets represent proposed (but not detected) intermediates; numbering according to Figure S5 (see SI).

Figure 4 Reconstructed LC-HR-MS ion chromatogram with the corresponding protonated exact masses indicating the given 5-MeO-2-Me-DALT metabolites in rat urine after 1 mg/kg BW dose administration; numbering according to Figures S1 and S2 (see SI).

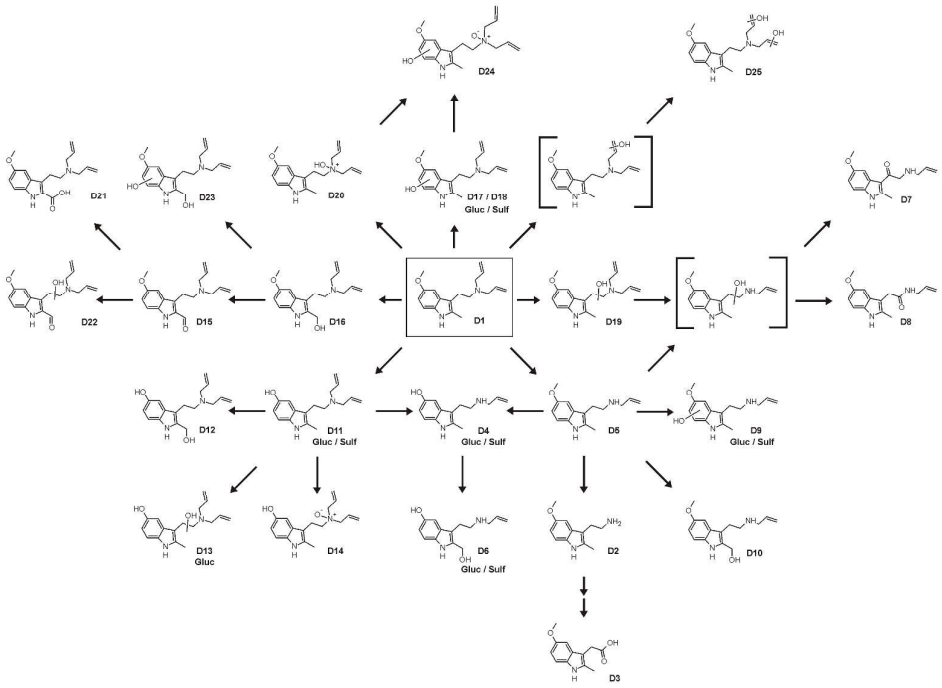

Figure 1 Proposed metabolic pathways of 5-MeO-2-Me-DALT. Phase II metabolites: glucuronides (G), and sulfates (S). Structures in brackets represent proposed (but not detected) intermediates; numbering according to Figure S1 (see SI).

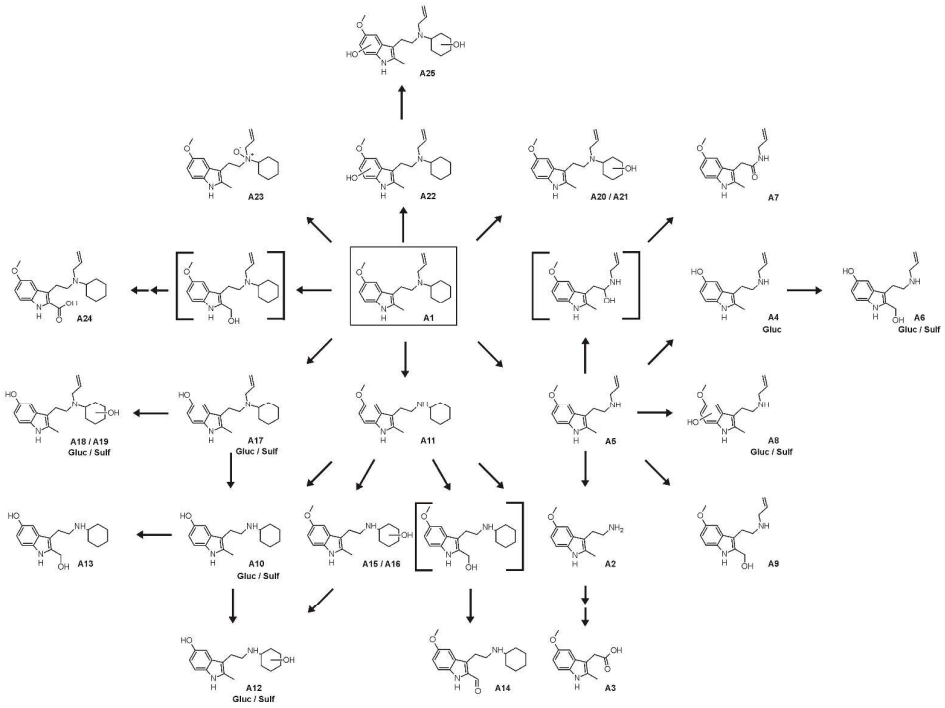

Figure 2 Proposed metabolic pathways of 5-MeO-2-Me-ALCHT. Phase II metabolites: glucuronides (G), and sulfates (S). Structures in brackets represent proposed (but not detected) intermediates; numbering according to Figure S3 (see SI).

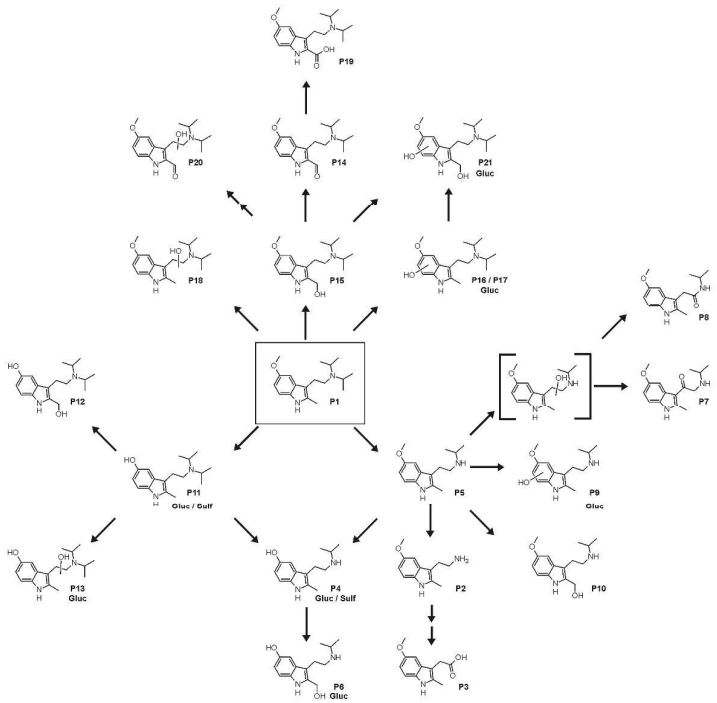

Figure 3 Proposed metabolic pathways of 5-MeO-2-Me-DIPT. Phase II metabolites: glucuronides (G), and sulfates (S). Structures in brackets represent proposed (but not detected) intermediates; numbering according to Figure S5 (see SI).

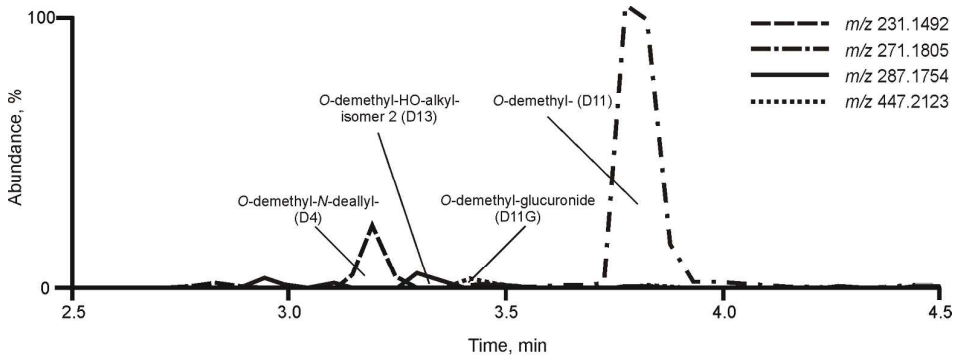

Figure 4 Reconstructed LC-HR-MS ion chromatogram with the corresponding protonated exact masses indicating the given 5-MeO-2-Me-DALT metabolites in rat urine after 1 mg/kg BW dose administration; numbering according to Figures S1 and S2 (see SI).